J. Korean Inst. Electr. Electron. Mater. Eng.
Vol. 36, No. 5, pp. 463-473 September 2023
doi: https://doi.org/10.4313/JKEM.2023.36.5.5
ISSN 1226-7945(Print), 2288-3258(Online)

Regular Paper

Recent Advances in a-IGZO Thin Film Transistor Devices: A Short Review

Jingwen Chen[1], Fucheng Wang[1], Yifan Hu[1], Jaewoong Cho[1], Yeojin Jeong[1], Duy Phong Pham[1], and Junsin Yi[2]

[1] Department of Electrical and Computer Engineering, Sungkyunkwan University, Suwon 16419, Korea

[2] College of Information and Communication Engineering, Sungkyunkwan University, Suwon 16419, Korea

(Received May 30, 2023; Revised June 22, 2023; Accepted June 25, 2023)

Abstract : In recent years, the transparent amorphous oxide thin film transistor represented by indium-gallium-zinc-oxide (IGZO) has become the first choice of the next generation of integrated circuit control components. This article contributes an overview of IGZO thin-film transistors (TFTs), including their fundamental principles and recent advancements. The paper outlines various TFT structures and places emphasis on the fabrication process of the active layer. The result showed that the size of the active layer including the length-to-width ratio and the width could have a significant effect on the mobility. And the process of TFT could influence the crystal structure of IGZO thin film. Furthermore, the article presents an overview of recent applications of IGZO TFTs, such as their use in display drivers and TFT memories. At last, the future development of IGZO TFT is forecasted in this paper.

Keywords: IGZO, Thin film transistor, Length-to-width radio, Process

NOMENCLATURE

TFT	Thin-film transistor
FET	Field-effect transistor
LCD	Liquid crystal display
OLED	Organic light-emitting diode
NVM	Non-volatile memory
IGZO	Indium-gallium-zinc-oxide
MOS	Metal oxide semiconductor
TAOS	Transparent amorphous oxide semiconductor
BTS	Bias temperature stress
NBTI	Negative bias temperature instability
BCE	Back-channel etched
ESL	Etch-stop layer
ISL	Insulated-stop layer
V_{th}	Threshold voltage
μ_{FE}	Field-effect mobility
SS	Subthreshold swing
PEALD	Plasma-enhanced atomic layer deposition
PECVD	Plasma-enhanced chemical vapor deposition
V_O	oxygen-vacancy
UV	Ultraviolet

✉ Duy Phong Pham; pdphong@skku.edu
Junsin Yi; junsin@skku.edu

Copyright ©2023 KIEEME. All rights reserved.
This is an Open-Access article distributed under the terms of the Creative Commons Attribution Non-Commercial License (http://creativecommons.org/licenses/by-nc/3.0) which permits unrestricted non-commercial use, distribution, and reproduction in any medium, provided the original work is properly cited.

1. INTRODUCTION

TFTs are a form of field-effect transistor (FET) that is extensively employed in electronic displays. TFTs first appeared in the 1960s. A Japanese business pioneered the technique for making liquid crystal displays (LCDs) at the time [1]. In the 1970s [2,3], IBM and Bell Laboratories started to develop thin-film transistor technology and established the current Metal-Oxide-Semiconductor (MOS) structure, which improved the reliability and stability of thin-film transistors. The need for high-resolution and high-brightness displays expanded dramatically as computer science advanced, resulting in the fast development of TFT-LCD display technology in the 1980s [2,3]. To date, an increasing number of TFT devices have been developed, and the technology has grown more frequently employed.

J. F. Wager et al. (2003) [2,4] initially suggested the concept of transparent electronics and published the transparent amorphous oxide semiconductor (TAOS) TFT-related research report represented by ZnO-TFT. Because this material has great electron mobility and electrical stability and can be manufactured at low temperatures, it offers a broad range of applications, such as LCD, active-matrix organic LCDs (AM-LCD), transparent electronic devices, and active-matrix liquid crystal display (AM-OLED). Nomura et al. [4] originally published their findings on the amorphous-IGZO (a-IGZO) TFT in 2001. The ZnO-based material is inexpensive and has excellent optical and electrical characteristics. Many researchers have published their findings regarding the a-IGZO TFT in recent years. Stefan (2018) [5] discovered a method to produce IGZO TFT at low temperatures, allowing this material to be applied to a flexible material. Chen et al. [6] investigated the characteristics of materials generated with various In_2O_3 cycle ratios in plasma-enhanced atomic layer deposition (PEALD) in 2023 and discovered that the optimal In_2O_3 cycle ratio is 35%. In the same year, Wu et al. [7] employed neutral oxygen beam irradiation (NOBI) to treat the IGZO layer. According to their findings, this method might be beneficial in reducing the intrinsic faulty condition.

With the advancement of technology, including TAOS, there are an increasing number of materials that might be utilized on the active layers of TFTs, such as organic materials [8], silicon layers [9-14], and so on [2]. However, TAOS TFT remains the most promising material for next-generation TFT devices. a-IGZO TFT provides the benefits of a thin film structure and low power consumption over standard transistors, allowing for high resolution, high brightness, rapid response, and low power usage. It is used in displays, for example, to regulate the flow of electric current, enabling each pixel to be switched on and off separately. Low power consumption was possible because of its unique construction.

Similarly, there are certain limitations to the application of a-IGZO material in TFT devices. In recent years, many scientists have conducted research on the reliability and stability of a-IGZO TFT, as shown in Table 1. Common reliability issues include bias temperature stress (BTS), electromigration, negative bias temperature instability (NBTI), stress migration, and more. Meanwhile, the a-IGZO film can also be influenced and restored by subsequent processes in the TFT fabrication process. The main reasons for these limitations are the defects at the interface between a-IGZO and other materials and the presence of oxygen vacancies within it, which will be discussed in detail in Section 3.2.

Table 1. Research of a-IGZO TFT limitation.

Year	Research topic	Key points
2023 [41]	Bias temperature instability	a-IGZO TFTs exhibit bias temperature instability under repeated stress and recovery conditions.
2023 [42]	External stress instability	Oxygen vacancies and the positively charged defects caused an abnormal negative shift in V_{TH} under PBTS.
2023 [43]	Positive bias stress instability	The interface defect and the subsequent atomic layer deposition (ALD) process play a role in the resistant of a-IGZO.
2023 [44]	Oxygen-related reaction	The ALD process results in the generation of a large number of oxygen vacancies at the interface between a-IGZO and the gate insulator layer.

This review paper contributes to a comprehensive understanding of fundamental a-IGZO device characteristics. Additionally, its manufacturing process, methodologies, and applications are discussed. Recent accomplishments of a-IGZO TFT devices are compiled in a table. It is anticipated that the assessment will reveal a general aspect of a-IGZO TFT technology that will be addressed in the subsequent version of the device. The structure of this review consists of the following sections:

a) The first section provides an introduction to materials and technologies.
b) Section 2 summarizes the material's fundamental theoretical characteristics.
c) Section 3 summarizes recent developments in a-IGZO TFT devices.
d) The fourth section discusses possible applications for a-IGZO TFT devices.

2. THE FUNDAMENTAL THEORETICAL ASPECT OF THE MATERIAL

2.1 Structure

TFTs are classified into four categories based on their gate structure: top-gate structure [15], bottom-gate structure [16-18], vertical-gate structure [3,19], and dual-gate structure [20]. A top-gate construction has the benefits of a simple manufacturing process, high reliability, superior current control ability, and low leakage current. The top-gate structure of IGZO TFTs, on the other hand, has a disadvantage in that the active layer is immediately exposed to the LCD screen's backlight, resulting in a decrease in the TFT devices' current characteristics. As a result, the bottom-gate structure is commonly employed in TFT LCDs. The opaque gate may prevent photo-generated carrier production in the active layer by blocking light from the backlight.

Bottom-gate structures are also classified as back-channel etched (BCE) [11,16-18] and etch-stop layer (ESL) or insulated-stop layer (ISL) [21]. Figure 1 depicts a BCE construction TFT [17]. Figure 1 depicts the BCE structure, with the bottom gate situated above the glass substrate and the active layer and passivation layer located above the bottom gate.

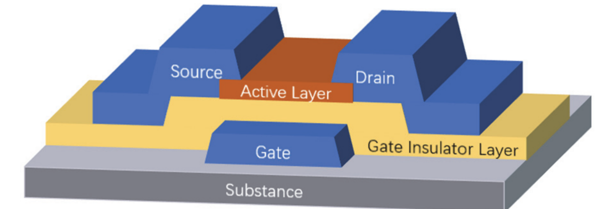

Fig. 1. The BCE structure TFT [17].

TFT, on the other hand, may be classified according to manufacturing techniques as conventional structure, semi-self-aligned structure [22], and self-aligned structure [23]. The semi-self-aligned structure [22] provides a guiding framework to accomplish layer alignment. The guiding framework may guarantee that various layers are aligned accurately. The self-aligned structure [23] is made possible by double-layer photolithography technology, which reduces alignment variance between layers and improves production accuracy as well as effectiveness.

2.2 Physical principles

The TFT, like other FETs, employs the gate to regulate the carrier in the channel to carry out the transistor's switching function. When a positive (+) voltage is subjected to the TFT's gate, as the n-type TFT which was illustrated in Fig. 2. [24],

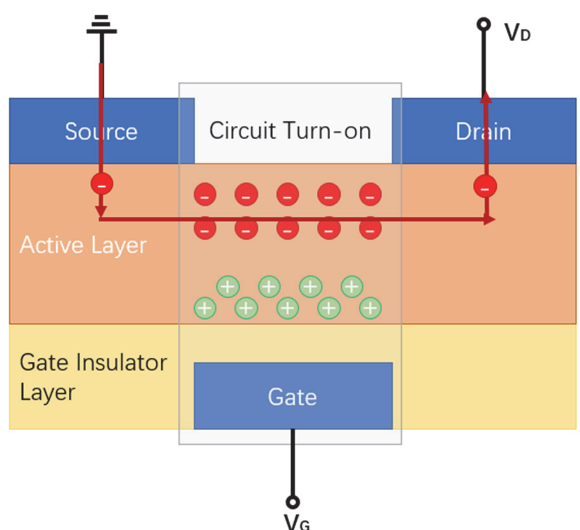

Fig. 2. Operating mechanism of n-type TFT [24].

electrons move close to the gate and accumulate due to the effect of electric field forces. The circuit is then turned on once a conductive channel is established between the source and drain electrodes. When a negative (-) voltage is applied to the gate, the electrons in the channel of the IGZO TFTs are depleted, resulting in the circuit being switched off.

TFTs have four essential electrical properties including threshold voltage (V_{th}) field-effect mobility (μ_{FE}), subthreshold swing (SS), and current switching ratio [25-27]. μ_{FE} is described as the average drift velocity of carriers under unit electric field intensity, or how quickly or slowly carriers move under electric field action. This option might represent the carrier's capacity to migrate. Zhang et al. (2016) [27] discovered that 1) the trapped charge between the active layer and the gate dielectric layer affects field effect mobility, 2) the difference in work function between the drain/source and the active layer is a critical factor in the operation of IGZO TFTs, 3) the defect charge in the active layer, 4) the material of the active layers, and so on. Hsieh et al. [25] presented a model for modeling the characteristics of an a-IGZO TFT in 2008. The deep-level defect in the band gap and the tail state defect in the band edge have a large influence on the μ_{FE} in their model.

2.3 The advanced IGZO active layer properties

TFT necessitates the deposit of a distinct active layer as a channel. A voltage is provided to the gate of IGZO TFTs to regulate channel conduction and blocking, which provides an electric field that regulates the accumulation and depletion of the majority of carriers in the channel. As a result, carrier mobility is one of the factors used to determine if a material is suitable for usage as a TFT channel material. Because of their comparable physical principles [28], a-Si: H and LTPS (Low-Temperature Poly-Silicon) were formerly prominent channel materials.

However, because of the physical features of silicon, these materials are readily impacted by covalent bonding [28]. The changes in the bond angle reflect a change in the electron energy level, resulting in certain high-density deep-tailed states. Amorphous-oxide-semiconductors (AOSs) that having post transition metal cations, in contrast to covalent semiconductors, are not susceptible to covalent bonding. Meanwhile, AOSs allow for processing at room temperature.

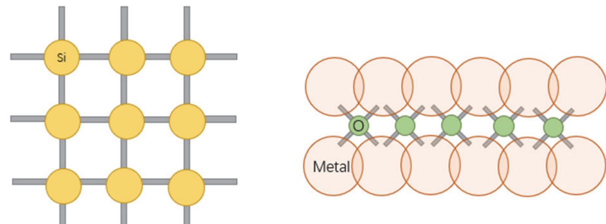

Fig. 3. The atomic structure model of covalent semiconductors (left) and AOSs (right) [28].

Indium Gallium Zinc Oxide (IGZO) is a well-known kind of AOS. The amorphous IGZO (a-IGZO) is an n-type semiconductor with strong field effect mobility among them. Another distinguishing feature of a-IGZO carrier transport is that when the Fermi level exceeds the mobility barrier, the Hall mobility of a-IGZO increases with increasing carrier concentration [28]. It denotes the presence of challenges in the conduction band when the carrier concentration is extremely low and electron mobility is constrained. However, when the carrier concentration exceeds the critical threshold, the barrier is broken and the Hall mobility increases considerably [27,28].

3. RECENT ADVANCES IN A-IGZO TFT DEVICES

The μ_{FE} of IGZO TFTs in the linear region differs from the μ_{FE} in the saturation region. We can use the following equations to simulate them:

Linear Region:

$$\mu = \frac{L}{W}\frac{g_m}{C_{OX}V_{DS}} \tag{1}$$

Saturation Region:

$$\mu = \frac{L}{W}\frac{2}{C_{OX}}\left(\frac{\partial\sqrt{I_{DS}}}{\partial V_{GS}}\right)^2 \tag{2}$$

3.1 Structure

Miniaturization of components is presently being researched to combine more components into the circuit board. However, as devices get smaller, the quantum impact and tunneling effect of semiconductors will become more

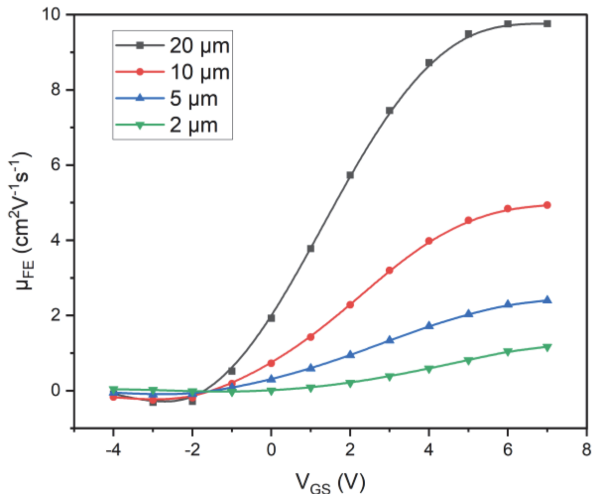

Fig. 4. The relationship between field effect mobility (linear region) and V_{GS} of IGZO TFT devices of different lengths and widths of 20 μm at 0.1 (V) of V_{DS} [29].

(a)

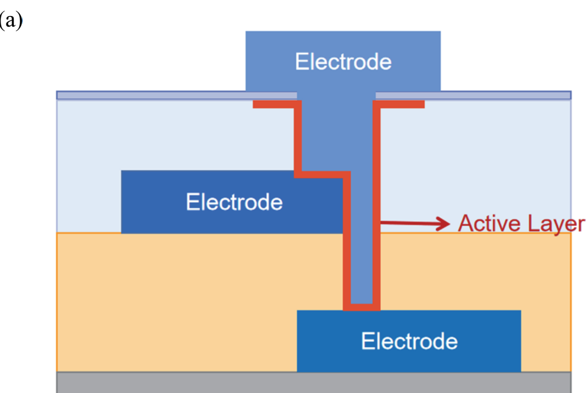

(b)

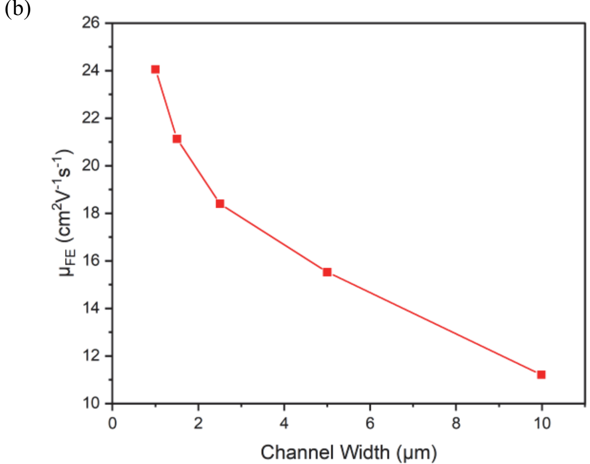

Fig. 5. (a)The trench-shaped vertical channel transistor and (b) the variation between μ_{FE} and the width of the channel [19].

important. As a result, mobility is closely related to the active layer's shape and size. Sharma et al. (2022) [29] established a straightforward mathematical model for an a-IGZO thin film transistor. Because they included an extra factor (V_C) in their model, this model might explain why to contact potential drops in short-channel devices. Figure 4 depicts the link between field effect mobility and VGS. According to their model, the normalized current (I_{DS}) flowing from the drain to the source rises as the channel length of IGZO TFTs grows. It is owing to the increased mobility of the field effect.

Ahn et al. (2022) [19] investigated a trench-shaped vertical channel transistor. With a one-step patterning procedure, trench structures were employed to establish the area of the vertical channel and source/drain contact in this structure [Fig. 5(a)]. The active IGZO layer was a 20 nm-thick film formed using the ALD technique at 200℃. Figure 5 on the right depicted the relationship between μ_{FE} and channel width. In this figure, as the width increased from 1 to 10 μm, the μ_{FE} decreased from 24.1 to 11.2 $cm^2V^{-1}S^{-1}$. Back-channel scattering effects might explain these results. These impacts would severely impede carrier movement.

More than one material can be used to form the channel layer. Guo et al. [30] researched the mobility of bilayer In_2O_3/IGZO transistors prepared by room-temperature pulsed layer deposition (PLD) in 2023. Figure 6 depicted the saturation mobility for various In_2O_3 thicknesses [Fig. 6(a)] and the linear mobility for various channel lengths [Fig. 6(b)]. The saturation mobility of TFT devices improved with the growth of In_2O_3 thickness, and the maximum saturation mobility is 47 $cm^2V^{-1}s^{-1}$. They demonstrated the relationship between mobility and channel length in Fig. 6(b) using the transfer-length method (TLM), also known as the transmission line technique. The mobility varies from 41 to 47 $cm^2V^{-1}s^{-1}$ at V_G = 30 V and V_D = 0.1 V. It can be inferred that: 1) the addition of the In_2O_3 layer might greatly boost TFT device mobility, and 2) TFT device mobility is favorably associated with channel length. The most essential aspect of all of this is that the high mobility is generated by an excellent percolation conduction channel and the oxygen vacancies, which are suppressed and may operate as defect states in the bilayer films.

(a)

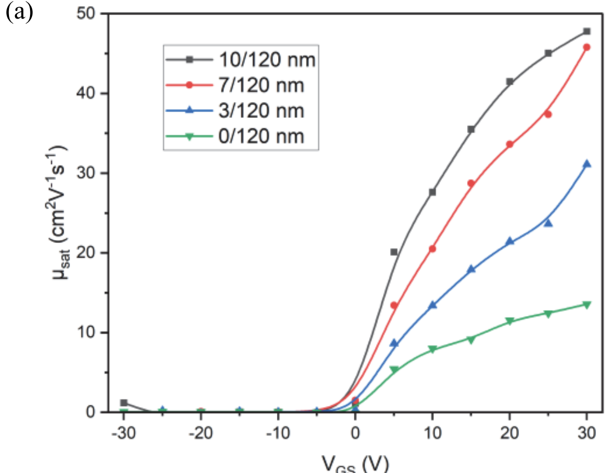

(b)

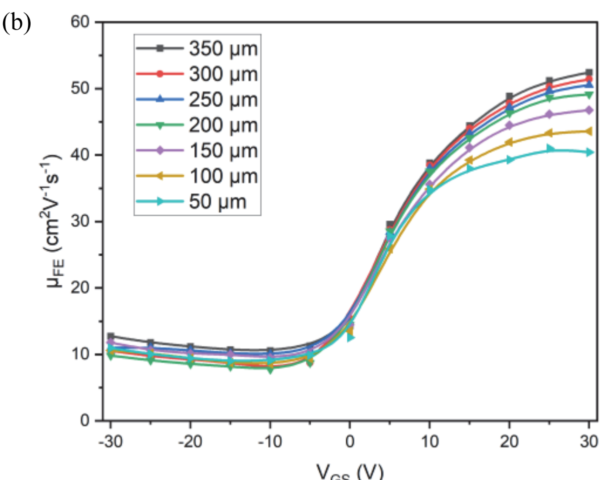

Fig. 6. (a) The saturation mobility of TFT transistors with different In_2O_3 film thicknesses and (b) the linear mobility of TFT transistors with different channel lengths [30].

3.2 Production technology

For large-scale integrated circuits and displays, the channel layers of TFT devices need to have the following advantages: 1) high mobility and good uniformity, and 2) high transmittance. High mobility devices could provide sufficient drive currents for large-scale liquid crystal displays. The devices that do not have good uniformity would easily be influenced by the defect states between crystalline grains and the interface states of the contact surface, and the quality of the film is poor. Concerning transmittance, this property is heavily influenced by the width of the band gap. The materials used for TFT devices are often wide-band gap materials.

The most common research method for mobility is to study the fabrication process of the channel layer. Different processes would have different effects on mobility. The Table 2 listed the materials and processes of TFT research in recent years.

In 2023, Wu et al. [7] reported their research about the IGZO transistor fabricated by AP-PECVD system with *in-situ* hydrogen plasma treatment. When the layers were treated by the H_2 plasma [31], the oxygen-vacancy (V_O) would be acted by hydrogen and formed V_O-H. In this structure, hydrogen serves as a shallow donor, which leads to an increase in mobility. Although plasma treatment can increase the mobility of IGZO TFTs, it can also introduce surface defects in the thin film. Therefore, oxidation using a neutral oxygen beam has become an increasingly important method for improving the performance of these TFTs. With the irradiation of the neutral oxygen beam, the oxygen particles would react with the surface/interface of the samples and form the oxygen-rich layers. In a-IGZO channel, the oxygen-deficient buried layer

Table 2. The materials and processes of TFT active layer in recent years.

Year	Materials of active layer	Processes	Mobility ($cm^2V^{-1}s^{-1}$)
2019 [45]	ZnO	H_2O_2 Oxidation Treatment	0.85
2023 [46]	a-InSnO	Low-temperature (150℃) annealing	70.53
2022 [47]	poly-In_2O_3:H	Low-temperature (300℃) solid-phase crystallization	139.2
2023 [6]	IGZO	PEALD	8.8
2023 [7]	a-IGZO	Treatment with neutral oxygen beam irradiation and *in situ* H_2 plasma	35
2023 [32]	IGZO	Sub-V operating Sn-doped for spin-coating	11.5

(a)

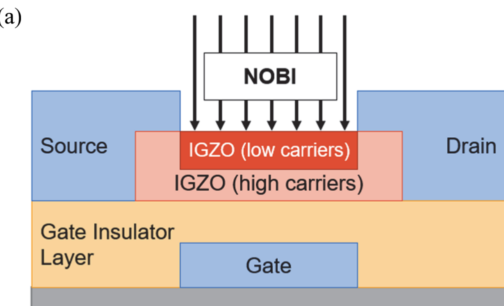

(b)

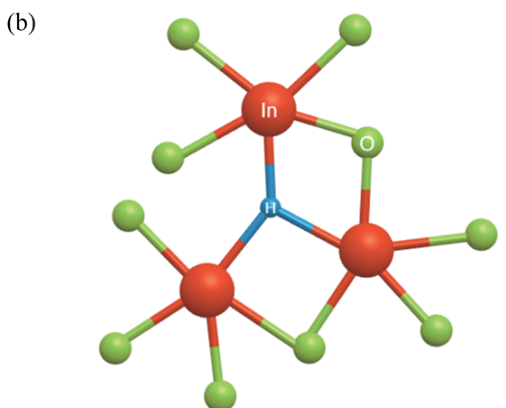

Fig. 7. (a) The saturation mobility of TFT transistors with different In_2O_3 film thicknesses and (b) the linear mobility of TFT transistors with different channel lengths [7,31].

would be left. Therefore, the quality of the transistor could be improved.

Park et al. (2023) [32] used a spin-coating technique to manufacture an active layer with a width/length (W/L) ratio of 1,000 μm/100 μm by adding stannum (Sn) to the IGZO precursor solution. Their research showed that the oxygen vacancies in IGZO are higher than in IGZTO (Sn-doped indium-gallium-zinc oxide). This TFT device showed great electrical performance such as the high μ_{eff} of 11.5 $cm^2V^{-1}s^{-1}$, which is nearly twice the mobility of the IGZO TFT. This showed that Sn doping could decrease the oxygen vacancy in IGZO thin film.

4. APPLICATIONS OF TFT

As a switching element in integrated circuits, IGZO TFT devices have been widely used over the years, such as display drivers [33,34], sensor applications [3], memory applications [34-38], and even neuromorphic systems [3]. In the field of display, TFT devices can control every pixel on the display screen, which has the characteristics of high performance and low power consumption. In other applications, TFT can be used to control the reading and writing of NVMS. This section will introduce some common applications of IGZO TFT.

4.1 Display drivers

a-IGZO TFT devices are suited for use in display drivers because of their high electron mobility, low-temperature manufacturing technique, and great uniformity across vast regions. The flexibility to utilize multiple substrates allows it to be used with OLED [33], LCD [34], wearable devices [3], and other items. Figure 8 shows the TFT-LCD process. Usually, there are four steps in the process including array, color film (CF), cell, and module. The TFT devices were deposited on the glass substrate in an array. And then, the color film was fabricated on another substrate. After that, the CF substrate and the array substrate would be combined in the cell process. These two substrates would be filled with liquid crystals, and each pixel would be aligned with a single transistor. Finally, add polarizing films on both sides of the substrate and install the circuit and backlight. A TFT-LCD screen is complete.

Wang et al. (2021) [34] researched the mechanism analysis of TFT-LCD pink mura. Pink mura is a kind of undesirable phenomenon in the process of production which refers to the pink phenomenon around the product after the TFT-LCD module continues to click the screen for a period of time in a high temperature and humidity environment. Their research showed that the pink mura occurs when a-IGZO TFT-LCD products are run for more than 500 hours in a humid environment. Although a-IGZO thin film possesses high electrical properties, water vapor also permeates through it at a high rate. It still needs to be studied how to correct this disadvantage.

Lai et al. [33] investigated a novel top-anode OLED/a-IGZO TFT pixel circuit based on top-emission 8K4K AM-OLEDs in 2019. The pixel circuit used in IGZO TFT-based displays allows for longer compensation times, which reduces the influence of mobility and makes it acceptable for both normally ON and normally OFF TFTs. In comparison to the typical 2T1C (two-transistor-one-capacitor) and 5T2C pixel circuits, the 4T2C circuit under consideration might lower

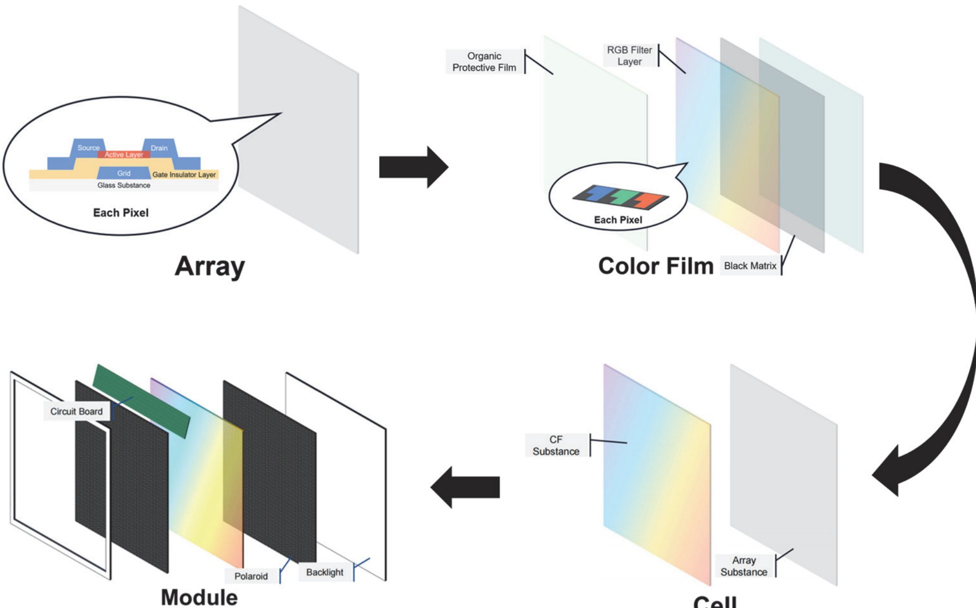

Fig. 8. TFT-LCD process.

current error rates to less than 5.79%.

4.2 Memory

With the development of TFT and System-on-Panel (SoP) technology, the pixel storage and storage blocks will be integrated directly onto a single display board to realize both data storage and power consumption reduction. More and more researchers focus on the TFT-based nonvolatile memory (TFT memory). Figure 9 showed the bottom gate structure TFT memory. Similar to traditional flash memories, TFT memory store data by controlling the amount of charge in the gate oxide layer. However, TFT memories which could not erase data by electrical method use light to erase data.

The TFT field effect influences the distribution of carriers in the Germanium-Antimony-Tellurium (GST) coating, and TFT resistance may replace the phase-change memory (PcRAM) reset resistance. Choi et al. [35] demonstrated in 2023 that parallel TFT-PcRAM could not only select or bypass PcRAM, but also control the memory's switching and resistance behavior. As a newer iteration of memory, TFT memory outperforms NAND Flash memory, as demonstrated by these findings.

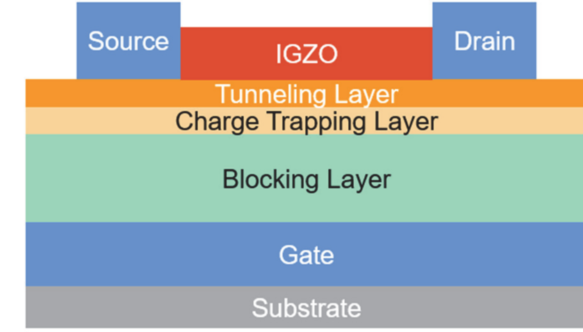

Fig. 9. Back gate structure TFT memory.

4.3 Flexible phototransistor

As a cutting-edge technology in modern science, flexible sensors possess the characteristics of being bendable and stretchable. Their flexibility and malleability allow for seamless integration with wearable device technologies, enabling applications such as medical health monitoring and sports tracking. Knobelspies et al. (2016) developed a flexible IGZO phototransistor that can be used for detecting ultraviolet (UV) light dosage [39]. The transistor utilizes a bottom-gate structure. The material has a bandgap of 3.05 eV and can

absorb wavelengths < 406 nm, covering the entire UV spectrum. By encapsulating the sensor in PDMS (approximately 100 μm thick), direct contact between the sensor and human skin is achieved without altering the optoelectronic properties of the transistor. The electrical wires can be directly connected to the readout device.

4.4 Binary neural network

XNOR operations in traditional binary neural networks require substantial circuitry for implementation. Lee et al. (2023) [40] proposed an alternative approach to replace XNOR operations with AND operations in certain parts of the network, aiming to reduce circuit complexity and power consumption. In addition, they incorporated TFT-type synaptic devices to implement this alternative approach in an effort to reduce the area and power consumption of the neural network's synaptic array. Compared to traditional methods, the proposed approach utilizing TFT-type synaptic devices can lower power consumption by approximately 25%. Their research indicates that this alternative approach somewhat reduces the accuracy of the network. However, it also brings significant advantages in terms of resource utilization and power consumption.

5. CONCLUSION

This article reviewed the basics of a-IGZO TFT devices and summarized the processes and technologies of IGZO TFT. The first section showed general aspects of the introduction to materials and technologies. The second part summarizes the basic theory and electrical characteristics of IGZO.

Section 3 discusses several methods to enhance the mobility of carriers in the active layer of TFTs. The research reveals that the structure, dimensions, and materials used in the active layer of TFTs have an impact on carrier mobility. The study also finds that by modifying the manufacturing process of the active layer, it is possible to influence the concentration of oxygen vacancies in IGZO material, thereby affecting its electrical performance.

Section 4 summarized some applications of IGZO TFTs. Researchers designed pixel circuits to increase circuit sensitivity and fault tolerance. And in the memory world, with the development of System-on-Panel technology, TFT-based nonvolatile memory will be a bright spot. Section 4 also provides a brief overview of the applications of TFTs in the field of neuroscience research and binary neural networks. IGZO TFTs are well-suited for amplifying and capturing weak signals due to their high carrier mobility, high visible light transmittance, high gain, and low noise characteristics. They enable the high-sensitivity acquisition of brain electrical signals. Furthermore, the utilization of TFTs in binary neural networks can significantly reduce the power consumption of the devices.

ORCID

Duy Phong Pham https://orcid.org/0000-0002-0512-4665
Junsin Yi https://orcid.org/0000-0002-6196-0035

ACKNOWLEDGEMENT

This work was supported by the National Research Foundation of Korea (NRF) grant funded by the Korean government (MSIT) (No.NRF-2022R1A4A1028702).

REFERENCES

[1] J. Liu, R. Liu, S. Zhan, Q. Luo, R. Chen, and X. Cheng, *IEEE Trans. Electron Devices*, **70**, 1682 (2023). doi: https://doi.org/10.1109/ted.2023.3241572

[2] J. Y. Kwon, D. J. Lee, and K. B. Kim, *Electron. Mater. Lett.*, **7**, 1 (2011). doi: https://doi.org/10.1007/s13391-011-0301-x

[3] Y. Zhu, Y. He, S. Jiang, L. Zhu, C. Chen, and Q. Wan, *J. Semicond.*, **42**, 031101 (2021). doi: https://doi.org/10.1088/1674-4926/42/3/031101

[4] K. Nomura, H. Ohta, K. Ueda, T. Kamiya, M. Hirano, and H. Hosono, *Science*, **300**, 1269 (2003). doi: https://doi.org/10.1126/science.1083212

[5] S. Knobelspies, B. Bierer, A. Daus, A. Takabayashi, G. A. Salvatore, G. Cantarella, A. O. Perez, J. Wöllenstein, S. Palzer, and G. Tröster, *Sensors*, **18**, 358 (2018). doi: https://doi.org/10.3390/s18020358

[6] Q. Z. Chen, C. Y. Shi, M. J. Zhao, P. Gao, W. Y. Wu, D. S. Wuu, R. H. Horng, S. Y. Lien, and W. Z. Zhu, *IEEE Electron Device Lett.*, **44**, 448 (2023). doi: https://doi.org/10.1109/led.2023.3239379

[7] C. H. Wu, S. K. Mohanty, B. W. Huang, K. M. Chang, S. J. Wang, and K. J. Ma, *Nanotechnology*, **34**, 175202 (2023).

doi: https://doi.org/10.1088/1361-6528/acb5f9

[8] Z. Cao, X. Huo, Q. Ma, J. Song, Q. Pan, L. Chen, J. Lai, X. Shan, and J. Gao, *Sens. Actuators, B*, **385**, 133685 (2023). doi: https://doi.org/10.1016/j.snb.2023.133685

[9] J. Choi, J. Cho, H. Kim, S. Jeong, T. Kim, S. K. Dhungel, Y. Kim, J. K. Song, Y. S. Kim, and D. P. Pham, *ECS J. Solid State Sci. Technol.*, **12**, 034001 (2023). doi: https://doi.org/10.1149/2162-8777/acbedd

[10] C. Liu, H. Zhou, Z. Jiang, and H. Xu, *Proc. 2019 IEEE 2nd International Conference on Electronics Technology (ICET)* (IEEE, Chengdu, China, 2019) p. 354. doi: https://doi.org/10.1109/ELTECH.2019.8839489

[11] G. Packard, R. G. Manley, and K. D. Hirschman, *ECS Trans.*, **90**, 79 (2019). doi: https://doi.org/10.1149/09001.0079ecst

[12] S. Lee, J. S. Park, and Y. Hong, *J. Korean Phys. Soc.*, **77**, 277 (2020). doi: https://doi.org/10.3938/jkps.77.277

[13] M. Moreno, A. Ponce, A. Galindo, E. Ortega, A. Morales, J. Flores, R. Ambrosio, A. Torres, L. Hernandez, H. Vazquez-Leal, G. Patriarche, and P.R.I. Cabarrocas, *Materials*, **14**, 6947 (2021). doi: https://doi.org/10.3390/ma14226947

[14] H. Xu, G. Wan, J. Mai, Z. Jiang, B. Liu, and S. Zhang, *Semicond. Sci. Technol.*, **38**, 035006 (2023). doi: https://doi.org/10.1088/1361-6641/acb2e8

[15] Y. Zhang, J. Li, J. Li, T. Huang, Y. Guan, Y. Zhang, H. Yang, M. Chan, X. Wang, L. Lu, and S. Zhang, *IEEE Electron Device Lett.*, **44**, 444 (2023). doi: https://doi.org/10.1109/led.2023.3237747

[16] T. Anutgan and M. Anutgan, *IEEE Trans. Electron Devices*, **68**, 6182 (2021). doi: https://doi.org/10.1109/ted.2021.3119540

[17] C. W. Kuo, T. C. Chang, J. J. Chen, K. J. Zhou, and T. M. Tsai, *IEEE Trans. Electron Devices*, **69**, 6789 (2022). doi: https://doi.org/10.1109/ted.2022.3217246

[18] C. Wang, C. Peng, P. Wen, M, Xu, L. Chen, X. Li, and J. Zhang, *IEEE Trans. Electron Devices*, **70**, 1687 (2023). doi: https://doi.org/10.1109/ted.2023.3244903

[19] H. M. Ahn, S. H. Moon, Y. H. Kwon, N. J. Seong, K. J. Choi, C. S. Hwang, J. H. Yang, Y. H. Kim, and S. M. Yoon, *IEEE Electron Device Lett.*, **43**, 1909 (2022). doi: https://doi.org/10.1109/led.2022.3210162

[20] S. H. Moon, S. H. Bae, Y. H. Kwon, N. J. Seong, K. J. Choi, and S. M. Yoon, *Ceram. Int.*, **48**, 20905 (2022). doi: https://doi.org/10.1016/j.ceramint.2022.04.082

[21] Y. F. Tu, C. L. Chiang, T. C. Chang, Y. H. Hung, L. C. Sun, C. W. Kuo, H. Y. Tu, H. C. Huang, and C. H. Lien, *IEEE Trans. Electron Devices*, **69**, 3181 (2022). doi: https://doi.org/10.1109/ted.2022.3166745

[22] S. K. Kim, Y. J. Choi, S. I. Cho, K. S. Cho, and J. Jang, *SID Symp. Dig. Tech. Pap.*, **29**, 379 (1998). doi: https://doi.org/10.1889/1.1833771

[23] J. Park, S. Choi, S. J. Myoung, J. Y. Kim, C. Kim, S. J. Choi, D. M. Kim, J. H. Bae, and D. H. Kim, *IEEE Electron Device Lett.*, **44**, 96 (2023). doi: https://doi.org/10.1109/led.2022.3225838

[24] H. Xie, *Ph.D. Mechanism Investigation and Process Development of Nitrogen-Doped Amorphous Oxide Semiconductor Thin Film Transistors*, Dissertation Submitted to Shanghai Jiao Tong University, 2018.

[25] F. M. Hossain, J. Nishii, S. Takagi, A. Ohtomo, T. Fukumura, H. Fujioka, H. Ohno, H. Koinuma, and M. Kawasaki, *J. Appl. Phys.*, **94**, 7768 (2003). doi: https://doi.org/10.1063/1.1628834

[26] H. H. Hsieh, T. Kamiya, K. Nomura, H. Hosono, and C. C. Wu, *Appl. Phys. Lett.*, **92**, 133503 (2008). doi: https://doi.org/10.1063/1.2857463

[27] G. Zhang, *Design and Researches on a-IGZO-Based TFT*, Telecommunication for the Degree of Master of Engineering, 2016.

[28] K. Nomura, H. Ohta, A. Takagi, T. Kamiya, M. Hirano, and H. Hosono, *Nature*, **432**, 488 (2004). doi: https://doi.org/10.1038/nature03090

[29] A. Sharma, P. G. Bahubalindruni, M. Bharti, and P. Barquinha, *Solid-State Electron.*, **192**, 108273 (2022). doi: https://doi.org/10.1016/j.sse.2022.108273

[30] M. Guo, H. Ou, D. Xie, Q. Zhu, M. Wang, L. Liang, F. Liu, C. Ning, H. Cao, G. Yuan, X. Lu, and C. Liu, *Adv. Electron. Mater.*, **9**, 2201184 (2023). doi: https://doi.org/10.1002/aelm.202201184

[31] H. K. Noh, J. S. Park, and K. J. Chang, *J. Appl. Phys.*, **113**, 063712 (2013). doi: https://doi.org/10.1063/1.4792229

[32] S. J. Park and T. J. Ha, *IEEE Electron Device Lett.*, **44**, 642 (2023). doi: https://doi.org/10.1109/led.2023.3243838

[33] P. C. Lai, C. L. Lin, and J. Kanicki, *IEEE Trans. Electron Devices*, **66**, 436 (2019). doi: https://doi.org/10.1109/ted.2018.2877945

[34] D. Wang, J. Y. Wan, D. Wang, R. H. Guo, H. M. Zhan, X. Chen, and X. B. Shao, *Chin. J. Liq. Cryst. Disp.*, **36**, 1264 (2021). doi: https://doi.org/10.37188/cjlcd.2021-0080

[35] W. Choi, G. Kim, H. Y. Kim, C. Yoo, J. W. Jeon, B. Park, G. Jeon, S. Jeon, S. Kang, Y. Lee, and C. S. Hwang, *ACS Appl. Electron. Mater.*, **5**, 1721 (2023). doi: https://doi.org/10.1021/acsaelm.2c01757

[36] M. M. Hasan, S. Roy, Mohit, E. Tokumitsu, H. Y. Chu, S. C. Kim, and J. Jang, *Appl. Surf. Sci.*, **611**, 155533 (2023). doi: https://doi.org/10.1016/j.apsusc.2022.155533

[37] L. Xu, J. Guo, C. Sun, Z. Zheng, Y. Xu, S. Huang, K. Han, W. Wei, Z. Guo, X. Gong, Q. Luo, L. Wang, and L. Li, *IEEE Electron Device Lett.*, **44**, 412 (2023).

doi: https://doi.org/10.1109/led.2022.3233824

[38] K. Yang, S. H. Kim, H. W. Jeong, D. H. Lee, G. H. Park, Y. Lee, and M. H. Park, *Chem. Mater.*, **35**, 2219 (2023). doi: https://doi.org/10.1021/acs.chemmater.2c03379

[39] S. Knobelspies, A. Daus, G. Cantarella, L. Petti, N. Münzenrieder, G. Tröster, and G. A. Salvatore, *Adv. Electron. Mater.*, **2**, 1600273 (2016). doi: https://doi.org/10.1002/aelm.201600273

[40] I. S. Lee, H. Kim, M. K. Park, J. Hwang, R. H. Koo, J. J. Kim, and J. H. Lee, *IEEE Electron Device Lett.*, **44**, 325 (2023). doi: https://doi.org/10.1109/LED.2022.3229321

[41] Y. Jeong, H. Kim, J. Oh, S. Y. Choi, and H. Park, *J. Electron. Mater.*, **52**, 3914 (2023). doi: https://doi.org/10.1007/s11664-023-10386-x

[42] C. H. Choi, T. Kim, M. J. Kim, S. H. Yoon, and J. K. Jeong, *IEEE Trans. Electron Devices*, **70**, 2317 (2023). doi: https://doi.org/10.1109/TED.2023.3261281

[43] J. Li, Y. Guan, J. Li, Y. Zhang, Y. Zhang, M. Chan, X. Wang, L. Lu, and S. Zhang, *Nanotechnology*, **34**, 265202 (2023). doi: https://doi.org/10.1088/1361-6528/acc742

[44] Y. Guan, Y. Zhang, J. Li, J. Li, Y. Zhang, Z. Wang, Y. Ding, M. Chan, X. Wang, L. Lu, and S. Zhang, *Appl. Surf. Sci.*, **625**, 157177 (2023). doi: https://doi.org/10.1016/j.apsusc.2023.157177

[45] B. Li, X. H. Gao, W. T. Zhang, T. Y. Wang, and B. C. Kim, *Comput. Knowl. Technol.*, **15**, 1009 (2019). doi: https://doi.org/10.14004/j.cnki.ckt.2019.1418

[46] M. Hu, L. Xu, X. Zhang, H. Hao, S. Zong, H. Chen, Z. Song, S. Luo, and Z. Zhu, *Appl. Phys. Lett.*, **122**, 033503 (2023). doi: https://doi.org/10.1063/5.0131595

[47] Y. Magari, T. Kataoka, W. Yeh, and M. Furuta, *Nat. Commun.*, **13**, 1078 (2022). doi: https://doi.org/10.1038/s41467-022-28480-9